



## Synthesis and evaluation of bivalent, peptidomimetic antagonists of the $\alpha_v\beta_3$ integrins

Feng Li<sup>a</sup>, Gouri S. Jas<sup>b</sup>, Guoting Qin<sup>a</sup>, King Li<sup>a,\*</sup>, Zheng Li<sup>a,\*</sup>

<sup>a</sup> Department of Radiology, The Methodist Hospital Research Institute, Houston, TX 77030, United States

<sup>b</sup> Department of Chemistry and Biochemistry, Baylor University, 101 Bagby Avenue, Waco, TX 76706, United States

### ARTICLE INFO

#### Article history:

Received 25 August 2010

Revised 3 September 2010

Accepted 7 September 2010

Available online 15 September 2010

#### Keywords:

Multivalency

Computer modeling

Integrin antagonists

### ABSTRACT

Targeting the integrin  $\alpha_v\beta_3$  by directly interfering with its function is considered to be an effective and non-cytotoxic strategy for the treatment of tumor. In this study, a series of bivalent analogs of peptidomimetic integrin antagonists IA **1** and IAC **2** were designed, synthesized, and evaluated for their ability to inhibit the integrin  $\alpha_v\beta_3$ . All the bivalent ligands exhibited increased potency compared to that of their monomeric counterparts for the integrin  $\alpha_v\beta_3$  with low nanomolar range binding affinity. The best bivalent ligand **6** tested in the series has an  $IC_{50} = 0.09$  nM evaluated by ELISA assay. We conclude that multivalency is providing a useful template for the development novel integrin  $\alpha_v\beta_3$  antagonists as potential therapeutics.

© 2010 Elsevier Ltd. All rights reserved.

The integrins are a family of cell-surface glycoproteins with critical roles in regulating both physiological and pathological processes. They are involved in a variety of cell signaling pathways by mediating cell adhesion, migration, and proliferation through explicit non-covalent interactions with endogenous extra cellular matrix (ECM) proteins.<sup>1</sup> 19 different integrin  $\alpha$  subunits and 8 different  $\beta$  subunits have been identified, forming at least 25  $\alpha\beta$  heterodimers and making the integrins a structurally and functionally diverse family of cell adhesion molecules.<sup>2</sup> One of the most important members of the integrin family is the integrin  $\alpha_v\beta_3$ , which is a heterodimeric transmembrane receptor protein that has been proven to be involved in the formation of angiogenesis, a phenomenon that occurs in major diseases such as cancer, osteoporosis, rheumatoid arthritis, and macular degeneration.<sup>3,4</sup> The distinct biological role of  $\alpha_v\beta_3$  makes it an attractive target for the development of therapies for a variety of diseases.<sup>5</sup> To date, six integrin inhibitors are being evaluated in clinical trials as anti-angiogenic agents for tumor imaging and therapy, which demonstrate remarkable affinity and selectivity to  $\alpha_v\beta_3$ .<sup>6</sup>

Design of new multivalent therapeutic and imaging agents has received a lot of attention because of their potential for increased binding affinity to biological receptors.<sup>7</sup> Bivalency, the most basic form of multivalency has already been adopted as a strategy in pharmaceutical research to improve interactions of designed ligands with natural receptors.<sup>8</sup> A peptidomimetic integrin  $\alpha_v\beta_3$  antagonist IA **1**, has been successfully exploited as the targeting

agent for gene delivery to angiogenic blood vessels (Fig. 1).<sup>9</sup> We also reported on IAC **2**, an IA carbamate derivative which enhanced the  $\alpha_v\beta_3$  binding affinity about 10 times in comparison with IA.<sup>10</sup> Using IA as the parent compound, we successfully developed a bivalent near-infrared fluorescent imaging probe with carbon chain linker which selectively targeted integrin  $\alpha_v\beta_3$  and showed promising *in vitro* and *in vivo* results for tumor detection.<sup>11</sup> Since the optimal linker plays an important role in multivalent ligand–receptor interactions we decided to explore this aspect of the formulation. In this study, we chose IA **1** and IAC **2** as parent compounds for the bivalent ligand construction employing rational structure design using computer simulation. Since polyethylene glycol (PEG) has low toxicity and immunogenicity, and has good solubility in both aqueous and organic solvents, it has been used as a carrier for various drugs. These favorable physicochemical properties make PEG a good linker material for constructing multivalent ligands. Herein we describe the synthesis of bivalent ligands **3–8** using PEG linker with different lengths to study structure function relationship using *in vitro* assays (Fig. 1).

The bivalent ligands **3–8** were synthesized using the procedure described in Figure 2, starting with commercially available triethylene glycol **9**, tetraethylene glycol **10**, and octaethylene glycol **11**. The PEGs were first activated as biscarbonylimidazoles derivatives **13–15**, and their chemical structure and purity was verified by NMR. The activated alcohols were then coupled to the free amine **1** and **2**, respectively, in DMSO to provide bivalent ligands **3–8**. All compounds were purified to homogeneity by semi-preparative RP-HPLC (Phenomenex C18 column), and their structures were confirmed by NMR and ESI ion trap mass spectrometry (Supplementary data).

\* Corresponding authors. Tel.: +1 28 17575518 (Z.L.).

E-mail addresses: [Kli@tmhs.org](mailto:Kli@tmhs.org) (K. Li), [Zli@tmhs.org](mailto:Zli@tmhs.org) (Z. Li).

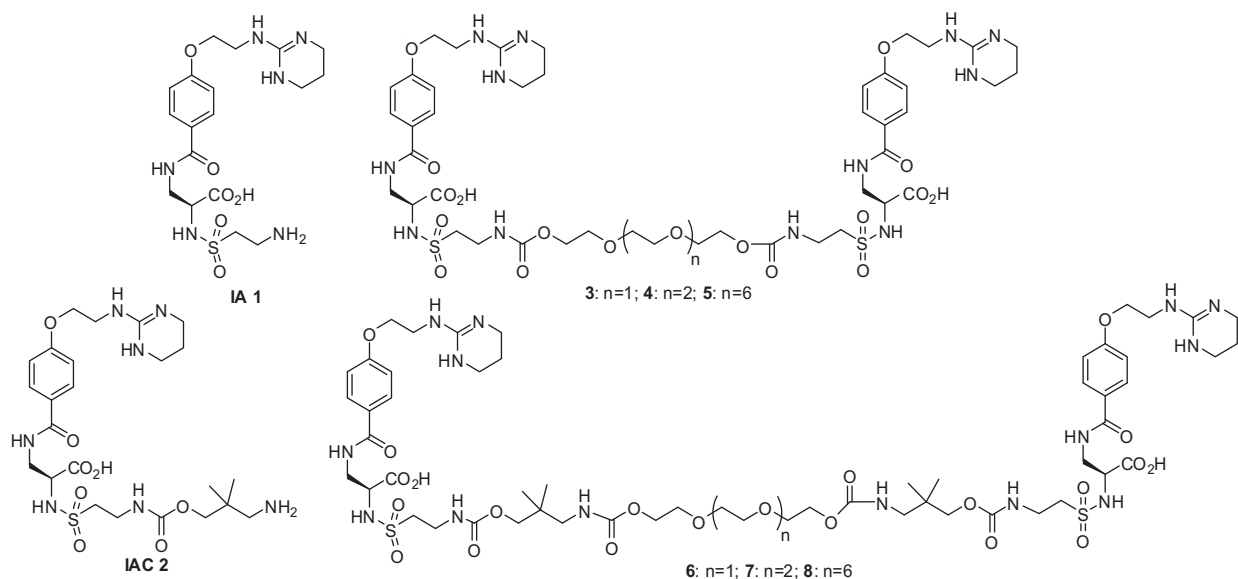


Figure 1. Schematic structure of IA 1, IAC 2, and bivalent ligands 3-8.

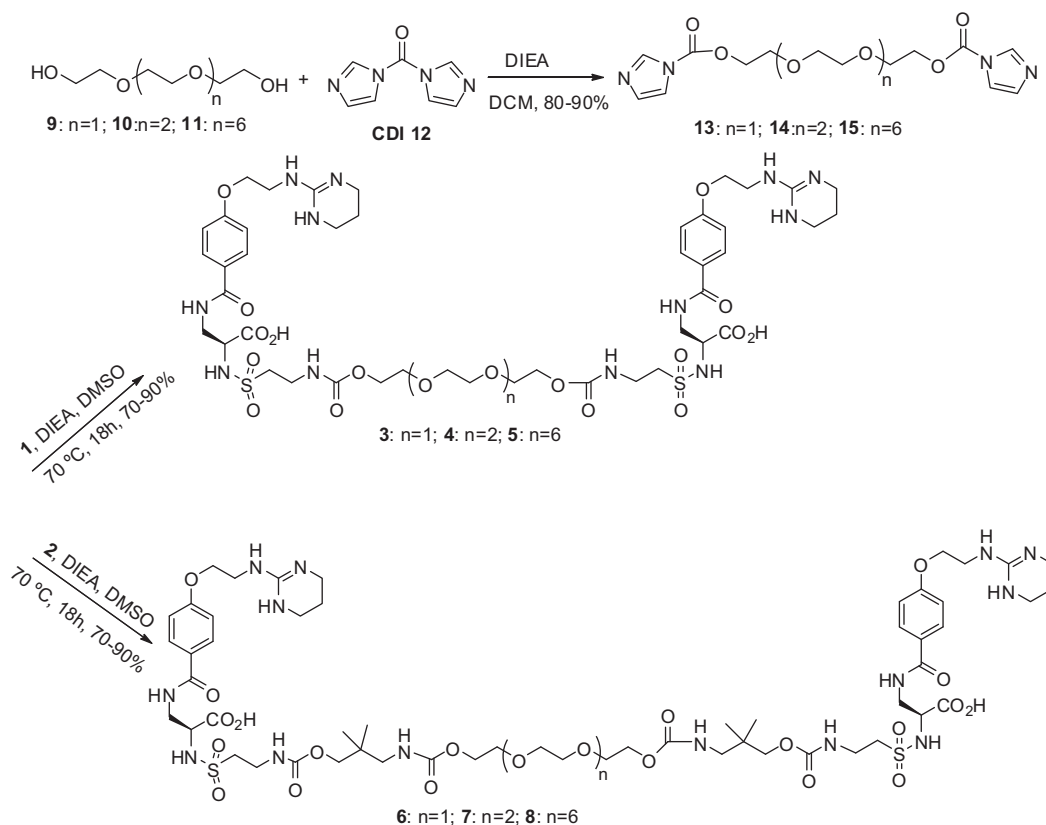


Figure 2. General procedure for the synthesis of bivalent ligands 3-8.

All final compounds were tested for their ability to competitively inhibit the attachment of the natural ligand vitronectin to purified human  $\alpha_v\beta_3$  by ELISA assay.<sup>12</sup> It measured competitive binding of the integrin antagonist and biotinylated human vitronectin for the immobilized receptor  $\alpha_v\beta_3$ . The results are listed in Table 1.

The computer modeling used molecular dynamics (MD) with explicit solvent. In the modeling study, bivalent IA and IAC with

varying linker lengths and compositions were constructed and molecular dynamics simulation was performed with CHARMM 35 force field (Supplementary data). From calculations of binding energies and ligand spatial distributions, the prediction of favored protein–ligand binding modes, interaction strengths, and binding specificity can be obtained with AutoDock simulations. Ten (10) LGA (Lamarckian genetic algorithm) docking runs were performed for each protein–ligand pair, with each run producing one possible

**Table 1**

In silico conformational energy and free energy of PEG-linked integrin antagonists and in vitro evaluation

Comps	<i>n</i>	In silico conformational energy (kcal/mol)	In silico free energy (kcal/mol)	In vitro ELISA IC <sub>50</sub> <sup>a</sup> (nM)
IA <b>1</b>	—	−17.0 (±2.0)	−3.1 (±0.8)	22.3 (±4.5)
IAC <b>2</b>	—	−41.5 (±2.0)	−10.2 (±1.6)	2.07 (±0.9)
<b>3</b>	1	−100.9 (±2.0)	−6.9 (±1.2)	0.16 (±0.12)
<b>4</b>	2	−98.0 (±2.0)	−6.1 (±1.2)	0.16 (±0.05)
<b>5</b>	6	−99.3 (±2.0)	−5.7 (±1.2)	0.16 (±0.10)
<b>6</b>	1	−140.9 (±2.0)	−8.2 (±1.2)	0.09 (±0.08)
<b>7</b>	2	−138.7 (±2.0)	−1.6 (±0.6)	0.11 (±0.02)
<b>8</b>	6	−153.4 (±2.0)	−2.1 (±0.6)	0.32 (±0.09)

<sup>a</sup> Values are averages of at least three determinations.

binding mode or solution. The solutions were first sorted in terms of the binding mode, i.e., the position and orientation of the ligand relative to the protein target. The solutions were clustered based on rms (root mean square) deviations in ligand atomic positions, with structures with rmsd of <0.5 Å grouped into a cluster. The total number of generated low-energy clusters measures the specificity of binding.<sup>13–16</sup> A small number of clusters indicates that the ligand has only a few possible binding modes and interacts with a specific site (or sites) on the target protein. On the other hand, a large number of clusters imply existence of a wide range of binding modes and lack of specific ligand–target interactions. The second step in sorting solutions involves identification of the solution of lowest binding energy within each cluster and ranking the different clusters according to this energy value. The solution with the lowest energy in the top-ranked cluster and all solutions with energies higher by up to 5.0 kcal/mol were considered as possible binding modes for ligand to target. The docking of each antagonist to the integrin  $\alpha_v\beta_3$  produced 3 clusters out of 10 runs. There were five solutions in the first cluster with an average docking energy of IA, IAC, and its dimers. A summary of the AutoDock results is presented in Table 1 and the docked structures of the first and second clusters are shown in Figure 3.

In general, all bivalent ligands **3–8** showed significantly improved affinity for the  $\alpha_v\beta_3$  as compared to monomer **1** and **2**. In

particular, bivalent ligands **3–5** (IC<sub>50</sub> = 0.16 nM) exhibited remarkable potency for the  $\alpha_v\beta_3$ , and showed 139-fold higher binding affinity as compared to that of the monomer **1** (IC<sub>50</sub> = 22.3 nM). Bivalent ligand **6** (IC<sub>50</sub> = 0.09 nM) had almost 23-fold higher affinity as compared to the corresponding monomer **2**. In fact, **6** is one of the most potent  $\alpha_v\beta_3$  antagonists reported to date (IC<sub>50</sub> = 0.09 nM). Although the binding affinity of parent monomer **2** is 10 times more potent than monomer **1**, the binding affinity of corresponding dimers did not show much difference. This observation suggests that the structure of the parent lead compound is not the only basis for the improved integrin  $\alpha_v\beta_3$  binding of the dimers. So, it is theoretically possible to design multivalent ligands with high binding affinity based on weak parent compounds. The hypothesis for the significantly increased binding affinity of dimers as compared to the corresponding monomer is that the local IA concentration is significantly ‘enriched’ in the vicinity of the neighboring integrin  $\alpha_v\beta_3$  sites. Once the first IA motif is bound to an integrin  $\alpha_v\beta_3$ , bivalency might lead to a faster rate of receptor binding and/or a slower rate of dissociation from the receptor. In computer modeling, the binding site defined by the cluster is in the cleft between the RGD binding domains in integrin  $\alpha_v\beta_3$ . It was observed that all the ligands stay at that site in the presence of the whole protein. This cluster presented the best model for a possible antagonist interaction to the integrin  $\alpha_v\beta_3$ . The modeling results

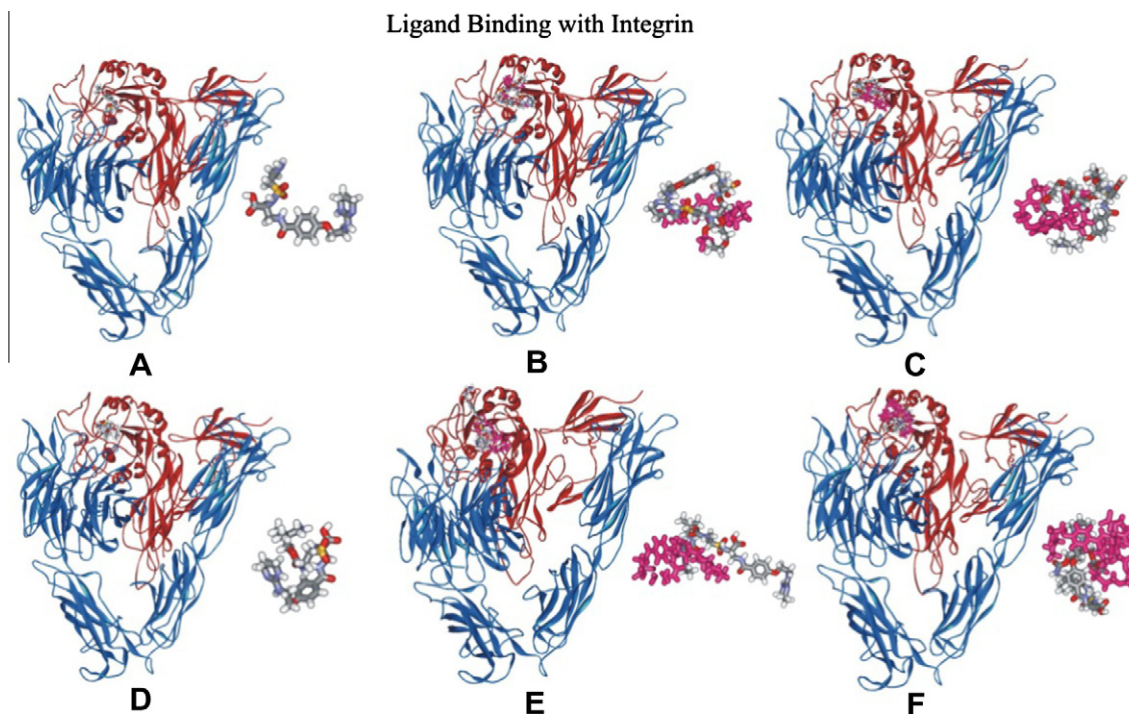


**Figure 3.** Binding of antagonists with the integrin. The corresponding structural antagonist conformations that are interacting with integrin are offset and enlarged to show molecular details. (A) IA monomer **1**, (B) IA dimer **4** (*n* = 2), (C) IA dimer **5** (*n* = 6), (D) IAC monomer **2**, (E) IAC dimer **7** (*n* = 2), and (F) IAC dimer **8** (*n* = 6).

suggested that IA dimers should have higher binding affinity than IA monomer because they have lower conformational energy and free energy compared with IA monomer. It also suggested IA dimers with PEGs linker ( $n = 1, 2, 6$ ) should have similar binding affinity because they have similar energy level in silico. Furthermore, among the bivalent conformations, the simulations suggest that IAC dimer **6** ( $n = 1$ ) has a higher specificity and better fit into the known active site than other conformations. The ELISA results correlates well with these predictions. However, ELISA results did not correlate perfectly with the molecular modeling results. For example, although IAC had the lowest free energy on computer modeling the ELISA result was much less impressive. The microscopic reason for these effects appears to be a lack of fit between different IA conformation and the inhibitor/substrate binding site. The docking results are approximate. The scoring is based on an empirical energy function, solvation effects treated with a highly simplified model, and only ligand flexibility taken into account, with the protein structure kept fixed.<sup>13–15</sup> Thus, the AutoDock results should only be considered as qualitative.

In summary, we have successfully designed and synthesized a series of bivalent antagonists of the  $\alpha_v\beta_3$  integrin through tethering IA and IAC with polyethylene glycol, respectively. Biological evaluation of six bivalent ligands shows that all dimers inhibit integrin  $\alpha_v\beta_3$  with increased potency as compared to that of their monomeric counterparts IA and IAC. The bivalent ligands **3–5** of IA with different linker length showed similar binding affinity for integrin  $\alpha_v\beta_3$  with  $IC_{50} = 0.16$  nM, 139 times higher in comparison with IA ( $IC_{50} = 22.3$  nM). In addition, the bivalent ligand **6**, with triethylene glycol linker, has the highest binding affinity in the series based on ELISA assay ( $IC_{50} = 0.09$  nM), the therapeutic study and development of these potent  $\alpha_v\beta_3$  integrin antagonists into imaging probes for optical and PET imaging is now in progress in our group.

#### Acknowledgment

This project was supported by The Methodist Hospital Research Institute, the M.D. Anderson Foundation, and the Vivian L. Smith Foundation.

#### Supplementary data

Supplementary data associated with this article can be found, in the online version, at doi:10.1016/j.bmcl.2010.09.035.

#### References and notes

1. Hynes, R. O. *Cell* **1992**, 69, 11.
2. Takagi, J.; Springer, T. A. *Immunol. Rev.* **2002**, 186, 141.
3. Folkman, J. *Nat. Med.* **1995**, 1, 27.
4. Schnitzer, J. E. *N. Engl. J. Med.* **1998**, 339, 472.
5. Arap, W.; Pasqualini, R.; Ruoslahti, E. *Science* **1998**, 279, 377.
6. Schottelius, M.; Laufer, B.; Kessler, H.; Wester, H. *Acc. Chem. Res.* **2009**, 42, 969.
7. Mammen, M.; Choi, S.-K.; Whitesides, G. M. *Angew. Chem., Int. Ed.* **1998**, 37, 2754.
8. Gestwicki, J. E.; Cairo, C. W.; Strong, L. E.; Oetjen, K. A.; Kiessling, L. L. *J. Am. Chem. Soc.* **2002**, 124, 14922.
9. Hood, J. D.; Bednarski, M.; Frausto, R.; Guccione, S.; Reisfeld, R. A.; Xiang, R.; Cheresch, D. A. *Science* **2002**, 296, 2404.
10. Burnett, C. A.; Xie, J.; Quijano, J.; Shen, Z.; Hunter, F.; Bur, M.; Li, K. C. P.; Danthi, S. N. *Bioorg. Med. Chem.* **2005**, 13, 3763.
11. Li, F.; Liu, J.; Jas, G. S.; Zhang, J.; Qin, G.; Xing, J.; Cotes, C.; Zhao, H.; Wang, X.; Diaz, L. A.; Shi, Z. Z.; Lee, D. Y.; Li, K. C. P.; Li, Z. *Bioconjug. Chem.* **2010**, 21, 270.
12. In vitro binding affinity assay: purified integrin  $\alpha_v\beta_3$  protein (Chemicon International, Temecula, CA) was applied to 96-well polystyrene microtiter plates at 1  $\mu\text{g}/\text{well}$ . After overnight incubation at 4 °C the plates were washed, and then blocked with milk solution (KPL, Inc., Gaithersburg, MD) at room temperature for 2 h. The blocking buffer was removed, and the plates were inoculated in quadruplicate with bivalent IAs with a typical starting concentration of 125 nM. Serial dilutions were prepared in the 96-well plates using multichannel pipettes. Biotinylated vitronectin solution (0.1  $\mu\text{g}/\text{well}$ ) was added to each well as a standard competitor. The plates were incubated at room temperature for 3 h, washed, and the bound vitronectin was detected using NeutrAvidin-HRP conjugate at 0.01  $\mu\text{g}/\text{well}$  (Pierce, Rockford, IL) and LumiGlo chemiluminescent substrate system (KPL, Inc., Gaithersburg, MD). The luminescence was read using a FLUOstar OPTIMA Microplate Reader (Durham, NC). The concentration of inhibitor producing 50% inhibition ( $IC_{50}$ ) of vitronectin binding to  $\alpha_v\beta_3$  was calculated based on a curve fitting model using KaleidaGraph 3.5 (Synergy Software, Reading, PA).
13. Goodsell, D. M.; Olson, A. J. *Proteins* **1990**, 8, 195.
14. Morris, G. M.; Goodsell, D. S.; Huey, R.; Olson, A. J. *J. Comput. Aided Mol. Des.* **1996**, 10, 293.
15. Morris, G. M.; Goodsell, D. S.; Halliday, R. S.; Huey, R.; Hart, W. E.; Belew, R. K.; Olson, A. J. *J. Comput. Chem.* **1998**, 19, 1639.
16. Xiong, J. P.; Stehle, T.; Zhang, R.; Joachimiak, A.; Frech, M.; Goodman, S. L.; Arnaout, M. A. *Science* **2002**, 296, 151.